EUROPEAN ORGANIZATION FOR NUCLEAR RESEARCH

CERN/EP 80-133
24 July 1980

DEEP INELASTIC MUON - NUCLEON SCATTERING AT HIGH Q^2

D. Bollini, P.L. Frabetti, G. Heiman, L. Monari and F.L. Navarria
Istituto di Fisica dell'Università, Bologna, Italy, INFN-Sezione di Bologna.

A.C. Benvenuti, M. Bozzo, R. Brun, H. Gennow, M. Goossens, R. Kopp,
F. Navach, L. Piemontese, J. Pilcher*, C. Rubbia and D. Schinzel
European Organization for Nuclear Research, CERN, Geneva, Switzerland

D. Bardin, J. Cvach, N. Fadeev, I. Golutvin, Y. Kiryushin, V. Kisselev,
M. Klein, V. Krivokhizhin, V. Kukhtin, W. Nowak, I. Savin, G. Smirnov,
G. Vesztergombi, A. Volodko and J. Zacek
Joint Institute for Nuclear Research, Dubna, USSR

D. Jamnik**, U. Meyer-Berkhout, A. Staude, K.M. Teichert,
R. Tirler, R. Voss and C. Zupancic
Section Physik der Universität, München, FRG

T. Dobrowolski, J. Feltesse, J.M. Malasoma, A. Milsztajn, J.F. Renardy,
Y. Sacquin, G. Smadja, P. Verrecchia and M. Virchaux
CEN, Saclay, France

(BCDMS Collaboration)

Presented by M. Klein

ABSTRACT

At the CERN SPS muon beam, deep inelastic cross sections have been measured in inclusive scattering of μ^+ and μ^- on carbon. In the region of $Q^2 = 40 - 100$ $(GeV/c)^2$ no systematic Q^2 dependence is observed for the μ^+/μ^- cross section ratio at 200 GeV beam energy. About 300.000 events at different energies are analyzed in terms of the structure function $F^2(X, Q^2)$ for $25 < Q^2 \lesssim 200$ $(GeV/c)^2$ and $0.2 < x < 0.7$.

Presented at the 20th International Conference
on High Energy Physics
Madison, Wisconsin, 16 - 23 July 1980

---

*) On leave from University of Chicago, U.S.A.

**) On leave from University of Ljubljana, Yougoslavia

1. INTRODUCTION

Deep inelastic lepton-hadron scattering has been very fruitful for the investigation of the nucleon structure. High momentum transfers Q^2 of $0(100)(GeV/c)^2$ probe the nucleon at distances of 10^{-15} cm where weak-electromagnetic interference effects are expected to reach the percent level.

The NA4 spectrometer was specially designed to cover the high momentum transfer region at the CERN SPS muon beam. Its basic features are therefore good acceptance at high Q^2 and high luminosity of $5 \cdot 10^{27}$ cm^{-2} per incoming μ reached with a 40 m long carbon target.

This report describes the spectrometer performance and the data analysis including a brief comparison of μ^+ with μ^- inclusive cross-sections. The structure function $F_2(x,Q^2)$ per nucleon was measured at E = 120, 200 and 240 GeV with about 80,000 events at each energy above Q^2 = 25, 40 and 50 $(GeV/c)^2$, respectively. The common result at all energies consists in a very weak Q^2 dependence. The x range of the data allows a determination of the moments of F_2 for $4 \leq n \leq 7$.

2. CHARACTERISTICS OF THE APPARATUS

The basic element of the NA4 muon spectrometer[1] shown in Fig. 1 is a magnetized iron torus which confines scattered muons up to $Q^2/s \sim 0.6$ ($s = Q^2_{max} = 2ME$). In focusing conditions muons perform oscillations with an amplitude proportional to Q^2/sB. The magnetic field B decreases from 2.1T to 1.7T towards the outer torus edge, the target being in a field free region. Calibration of the iron torus is essential for the reliability of the results. Deflecting beams of known energy directly into the torus, the incoming energy has been reconstructed to better than one per cent. The measured momentum resolution is 7%, mainly due to multiple scattering in the iron.

The spectrometer is made of ten identical iron toroids (supermodules) with interspersed liquid scintillation counters (TC) and multiwire proportional chambers to detect and track the scattered muons (see Fig. 1) The

trigger requires any set of four consecutive TC planes in coincidence with the beam, not vetoed by the beam halo counters in front of the set-up. The ring structure of the TC's allows preselection of the minimum Q^2 by requiring that the scattered muon traverses the counter above a given ring. The periodicity of the set-up provides redundant trigger information which allows a determination of the triggering efficiency (98% for the data presented). As an example, Fig. 2 displays a deep inelastic event recognized at several places along the apparatus.

The incoming beam has an energy spread of ±4%. A set of beam hodoscopes before and after a bending magnet in the beam ("beam momentum station" in Fig. 1) determines the individual primary energy with a resolution of 5%. Inside the apparatus the beam is defined by five hodoscopes. The beam profile has a $\sigma_x \sim \sigma_y$ of 2 cm (Fig. 3a) well inside the inner 48 hodoscope elements (Fig. 3b). The dashed circle in Fig. 3b indicates the 6 cm target radius.

3. DATA REDUCTION AND μ^+-μ^- COMPARISON

The data described here, about 5% of the statistics on tape, were taken in 1979 at energies*) of 120, 200 and 240 GeV with a trigger rate of 10^{-5} triggers/gated μ at beam intensities of, typically, 10^7 μ/pulse. After track reconstruction and momentum fit, events above p = 15 GeV are accepted if the reconstructed track gives a valid trigger pattern. Eye scanning of about 10% of the events verified the automatic event selection to be correct at the level of 10^{-2}. Examples for possible errors at this level are residual halo feed through, reconstruction ambiguities or accidentals.

At 200 GeV a short test run was performed with the beam polarity (and helicity) changed from μ^+ to μ^-. The torus field was reversed correspondingly in order to maintain the focusing condition. The μ^- intensity was about $5 \cdot 10^6$ μ/pulse, twice lower than for μ^+. Figure 4 shows the

---

*) Data at the highest available muon energy of 280 GeV are being analyzed and are not included in this report.

Q^2 distribution of μ^+ events, not corrected for acceptance, and the μ^-/μ^+ cross-section ratio. No systematic trends can be observed beyond the statistical accuracy, neither for Q^2 nor for other variables like momentum, angle or vertex position. Thus for the analysis of $F_2(x,Q^2)$ the μ^+ and μ^- samples have been combined.

4. $F_2(x,Q^2)$

The Monte Carlo simulation of the experiment takes into account the beam phase space, energy loss, multiple scattering, δ rays accompanying the track and hadronic showers. Tracks are reconstructed and fit using the same program as for the data. The trigger in the Monte Carlo is simulated including the small inefficiencies in the detector and electronics which are determined from the data. Figure 5 shows lines of 40% acceptance in the Q^2/Q^2_{max} - y plane ($y = \nu/E$ the relative energy transfer), which basically reflect the scale invariance of the track oscillation amplitude.

Extracting the one-photon exchange cross-section requires a correction for higher order processes. Figure 6 shows the leptonic vertex corrections to first order in α [2] which amount to a few per cent (solid curves) except near $y = 1$. The data are also corrected for weak-electromagnetic interference effects which for μ^+ have the tendency to compensate for the Q^2 dependence of the radiative contribution (dashed curves calculated in the WS/GIM theory).

Figures 7a and b contain the measurements of $F_2(x,Q^2)$ at 120, 200 GeV and 200, 240 GeV, respectively. The structure functions are given at the bin centre for x (0.2, 0.7) and with statistical errors only. The results at different energies are in good agreement with an estimated relative normalization error of 5%. At the low Q^2 and low x boundaries of the kinematic region the errors are still dominated by systematics as indicated by the extra error bars in Fig. 7. Control of the absolute momentum calibration to about 0.5% and edge effects of the acceptance imply systematic errors of about 10 - 15% at low Q^2/s and decreasing towards higher Q^2. Their detailed contributions have not yet been finally assessed and the quoted values reflect the current status of the analysis rather

than the intrinsic limitations of the experiment. Combination of 120 GeV with the 200 and 240 GeV data would require a knowledge of the Q^2,x behaviour of R, at least at $x \lesssim 0.4$. This is illustrated in Fig. 8 giving the ratio of two structure functions with R = 0.22 and R = 0 at 120 GeV and 200 GeV. The results in Fig. 7 are given for R = 0, the effect of changing R from 0 to 0.2 being still smaller than the systematic uncertainties.

As can be seen from Fig. 7 the observed Q^2 dependence is very weak, indicating that any mass scales for the strong interaction are small compared to the Q^2 values involved ($Q^2 > 25$ (GeV/c)^2). Simple parametrizations of the type $\sum_{i=1}^{3} a_i (1 - x)^{i+x} (1 + C \ln Q^2/3 \ln 1/4x)$ only slightly favour the presence of the Q^2 dependent term with $C = 0.12 \pm 0.03$ (statistical error).

In the covered x region, moments of F_2 can be calculated for $4 \leq n \leq 7$. The integrand is extrapolated to the edges averaging over the results due to an overall fit to F_2 and to fits in slices of Q^2. The n,Q^2 region of the moments presented in Fig. 9 is determined by the requirement that 2/3 of the integrand has to be given by the data. The quoted error combines the statistical error with 20% of the extrapolation contribution. Elastic and resonance combinations are negligible for $Q^2 > 25$ (GeV/c)^2. The resulting moments are compatible with the trend observed by CDHS[3] from the combination of neutrino and electron data (open points in Fig. 9), but add substantially to the high Q^2 region.

The data presented here, while less than 5% of the final sample, have the statistical power to quantify the pattern of scaling violations at high Q^2. While we have no direct indication of large systematic errors, we cannot rule out their existence at the present stage of our analysis. It is clear that scale breaking is small for $Q^2 > 25$ (GeV/c)^2 and control of systematic effects to the level of a few per cent becomes vital. We defer a discussion of the implications of these data for theories of the strong interaction, until additional cross checks have been performed on systematic effects.

REFERENCES

1) A detailed description of the spectrometer has been given in, D. Bollini et al., "Deep Inelastic Muon Scattering on Carbon at Large Q^2", Proc. of the Lepton-Photon Symposium, Fermilab 1979, p. 149.

2) A.A. Akhundov, D.Yu. Bardin and N.M. Shumeiko, Jad. Fiz. 26 (1977) 1251.

3) J. de Groot et al., Phys. Lett. 82B (1979) 292.

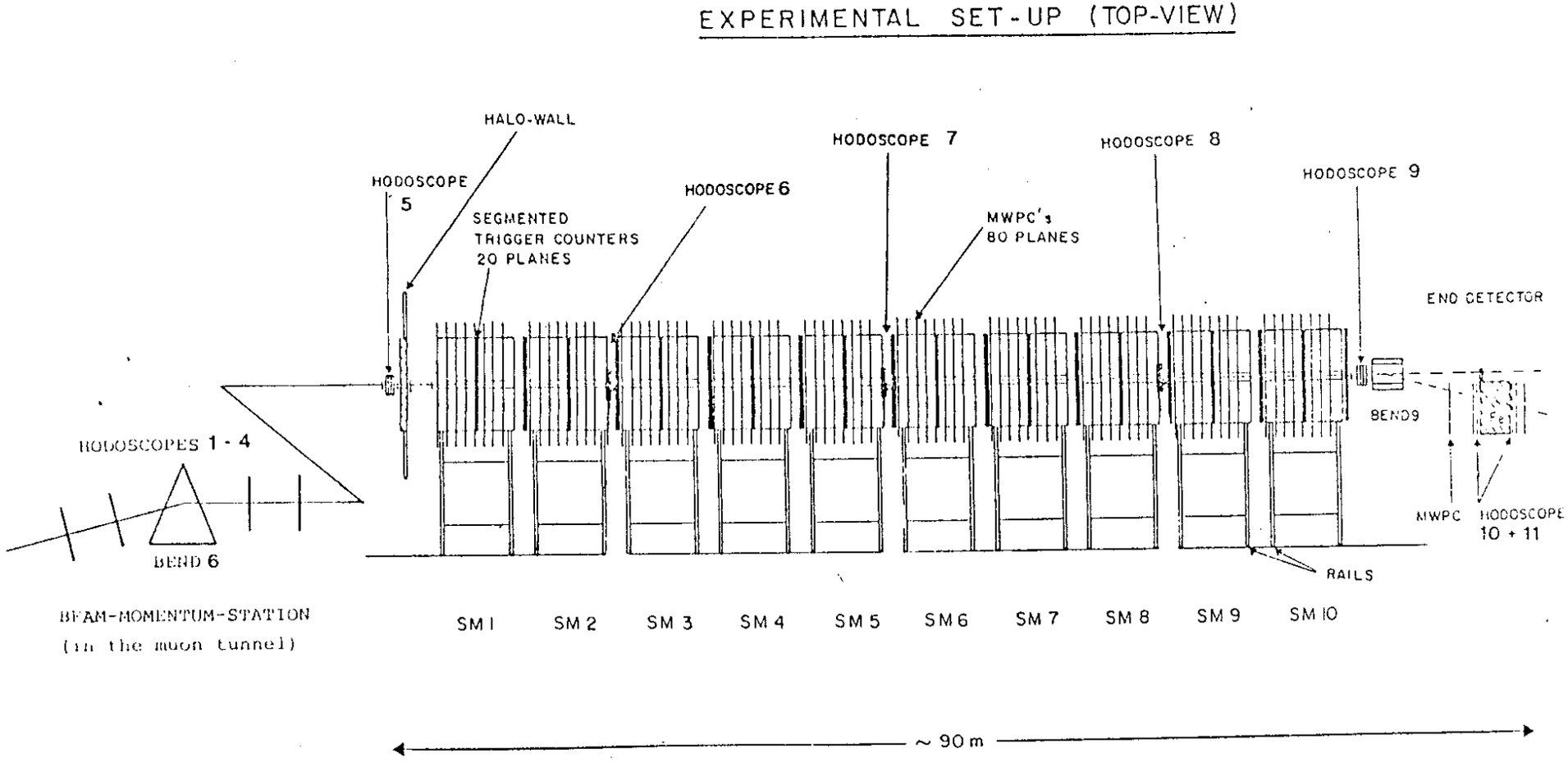
EXPERIMENTAL SET-UP (TOP-VIEW)
HALO-WALL
HODOSCOPE 5
SEGMENTED TRIGGER COUNTERS 20 PLANES
HODOSCOPE 6
HODOSCOPE 7
MWPC's 80 PLANES
HODOSCOPE 8
HODOSCOPE 9
END DETECTOR
BEND9
MWPC
HODOSCOPE 10 + 11
RAILS
HODOSCOPES 1 - 4
BEND 6
BEAM-MOMENTUM-STATION
(in the muon tunnel)
SM 1
SM 2
SM 3
SM 4
SM 5
SM 6
SM 7
SM 8
SM 9
SM 10
~ 90 m

FIG.1

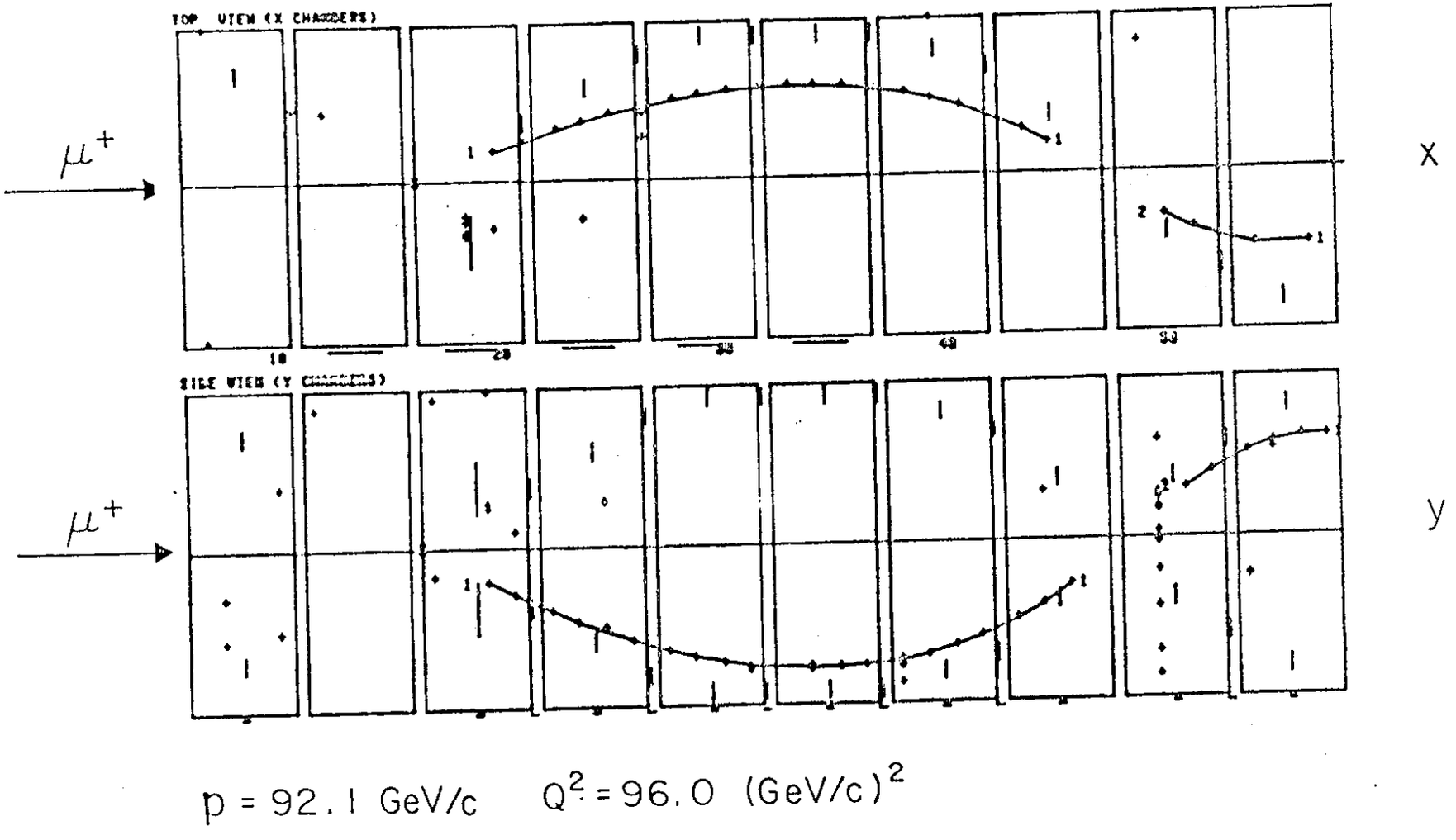

Fig. 2 Deep inelastic event in x and y projection with two oscillations. The horizontal bars below supermodules 2 to 6 in the top view mark the five triggers fired by the event.

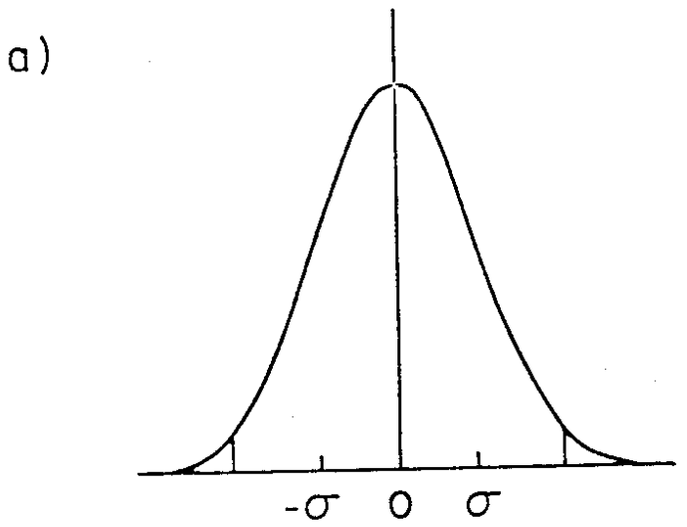

Fig. 3a Beam profile at the entrance to the target

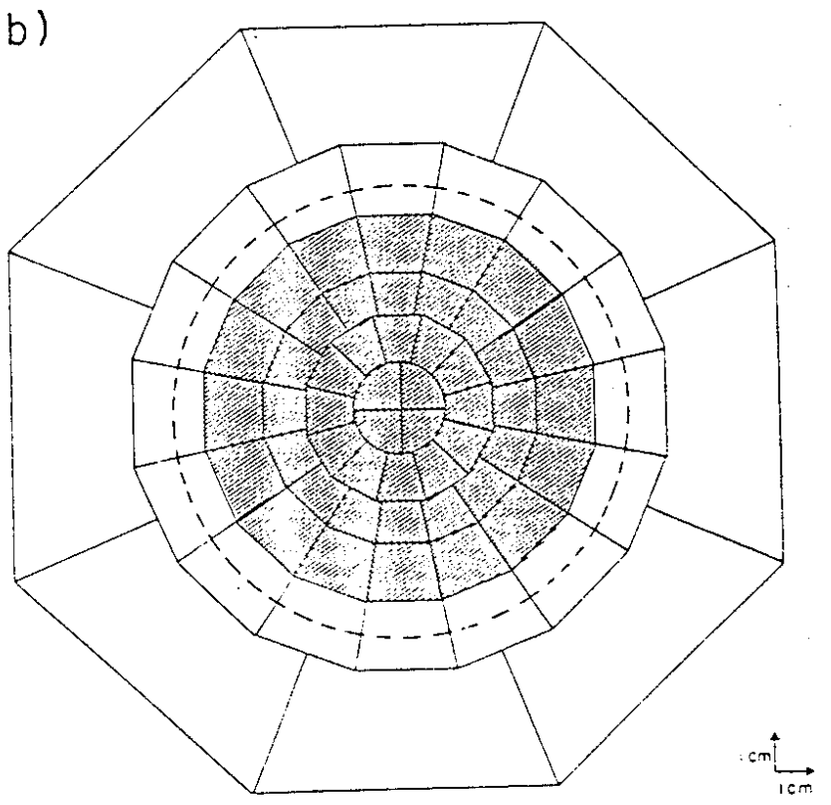

Fig. 3b Hodoscope mosaic structure as seen by the beam. The 48 inner elements of Hodoscope 5 (see Fig. 1) define the beam inside the spectrometer. The dashed circle indicates the 6 cm target radius.

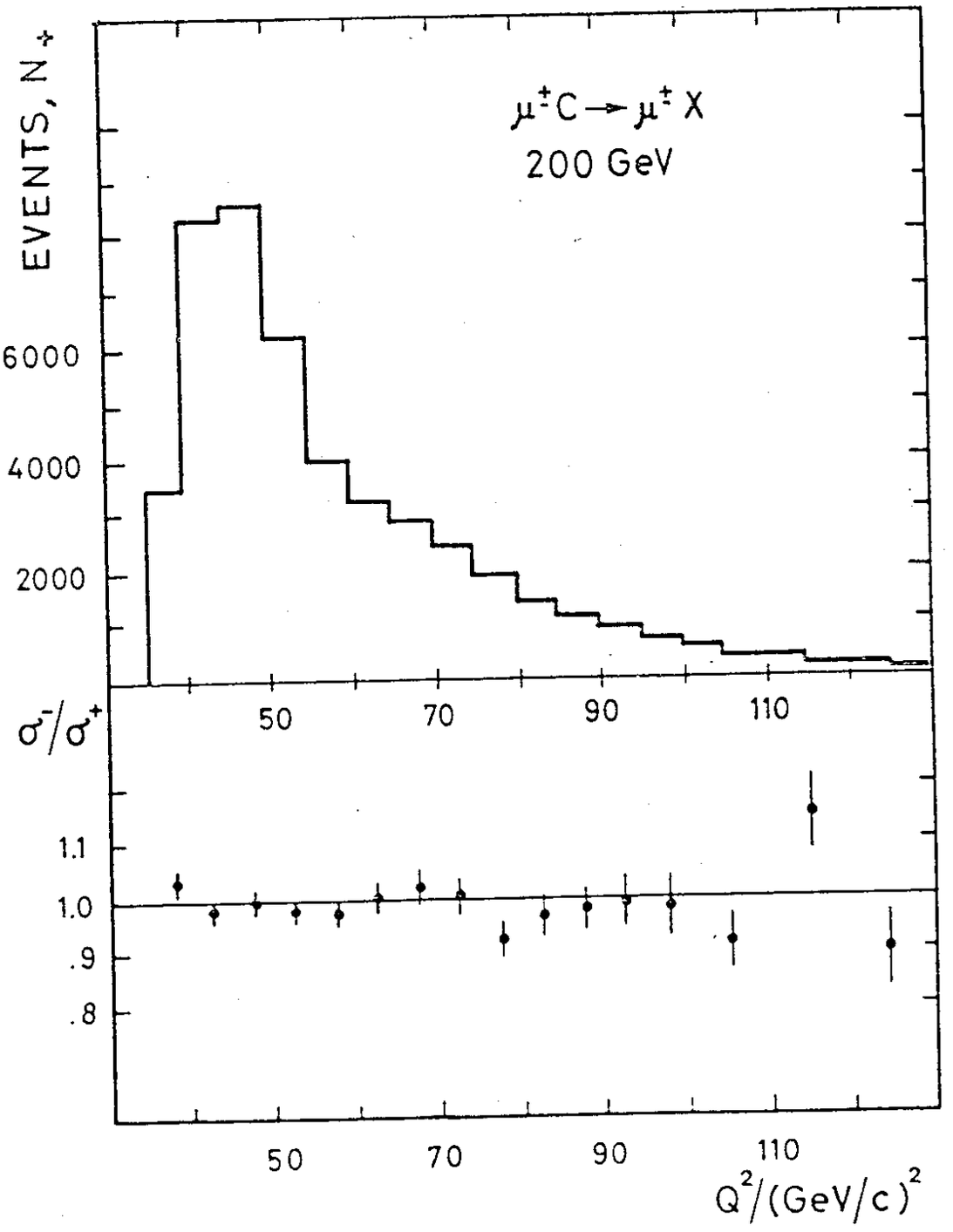

Fig. 4 Q^2 distribution of μ^+ events, not corrected for acceptance, and μ^-/μ^+ cross-section ratio at 200 GeV incoming energy

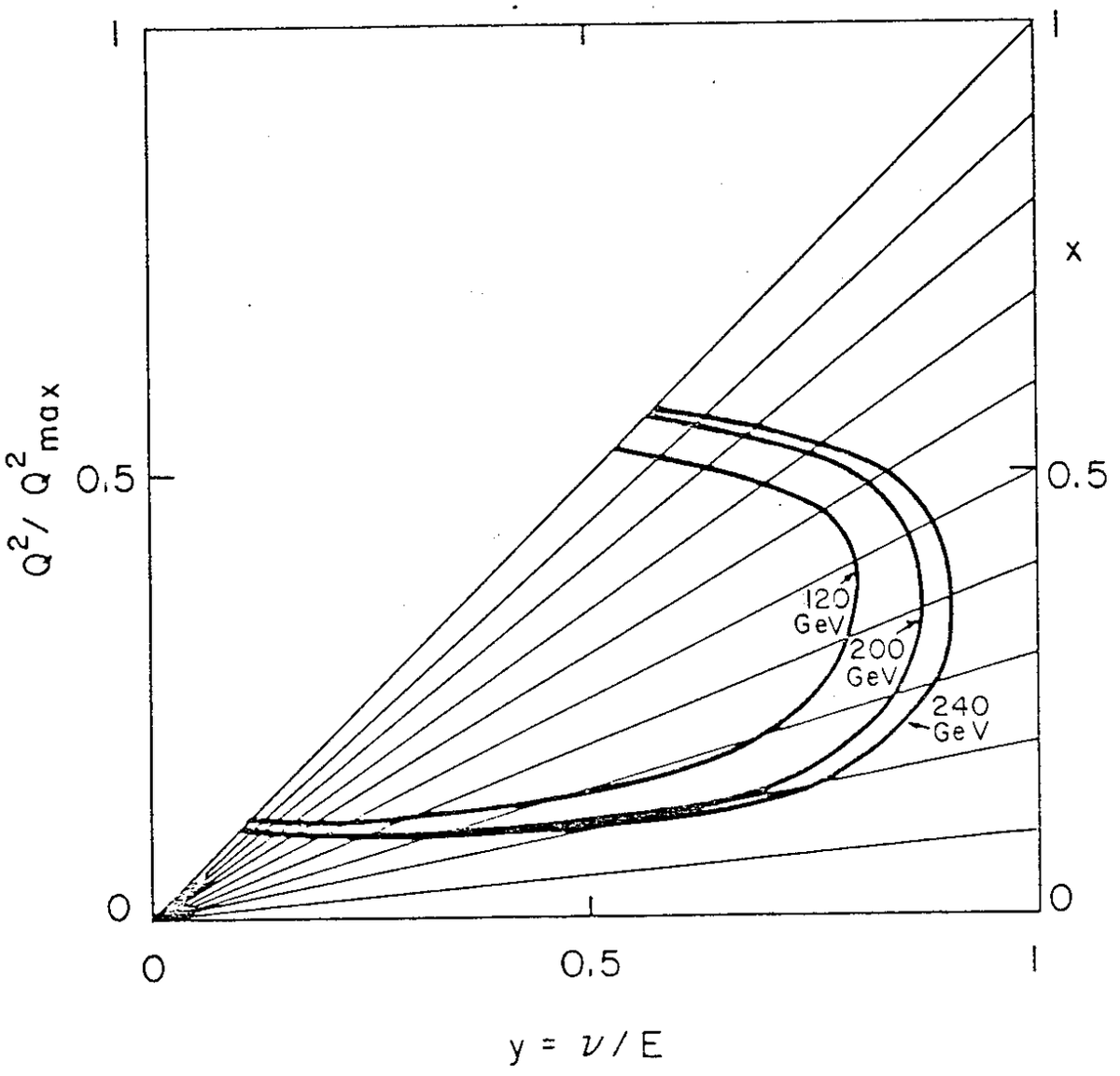

Fig. 5 40% acceptance contours in the Q^2/Q^2_{max} - y plane at 120, 200 and 240 GeV

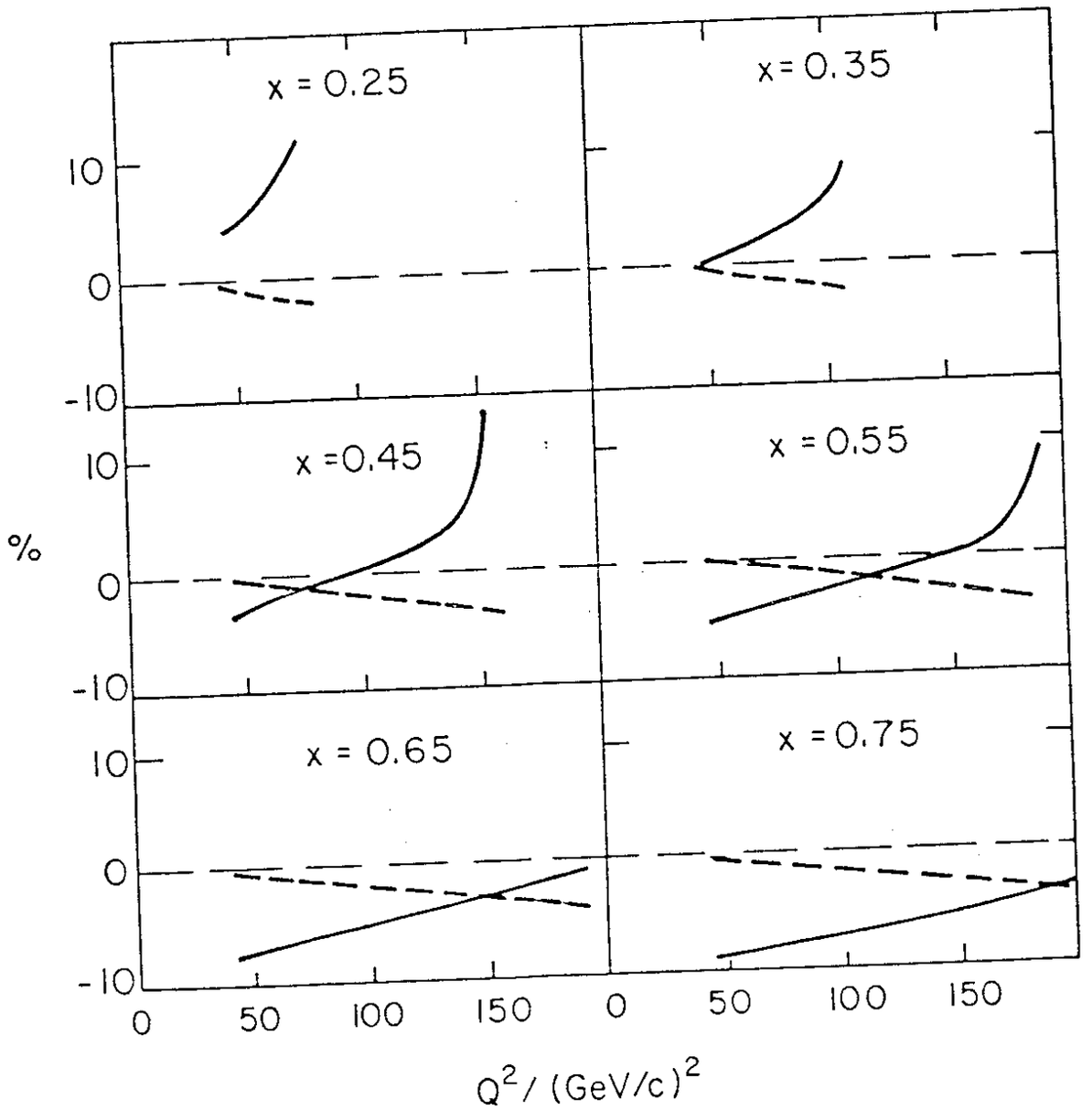

Fig. 6 Corrections for higher order processes in per cent. Solid curves: radiative corrections to order α at the leptonic vertex[2]. Dashed curves: weak-electromagnetic interference contribution calculated in the WS/GIM theory for μ^+, $\sin^2\theta = 0.23$ and a beam helicity of -0.8.

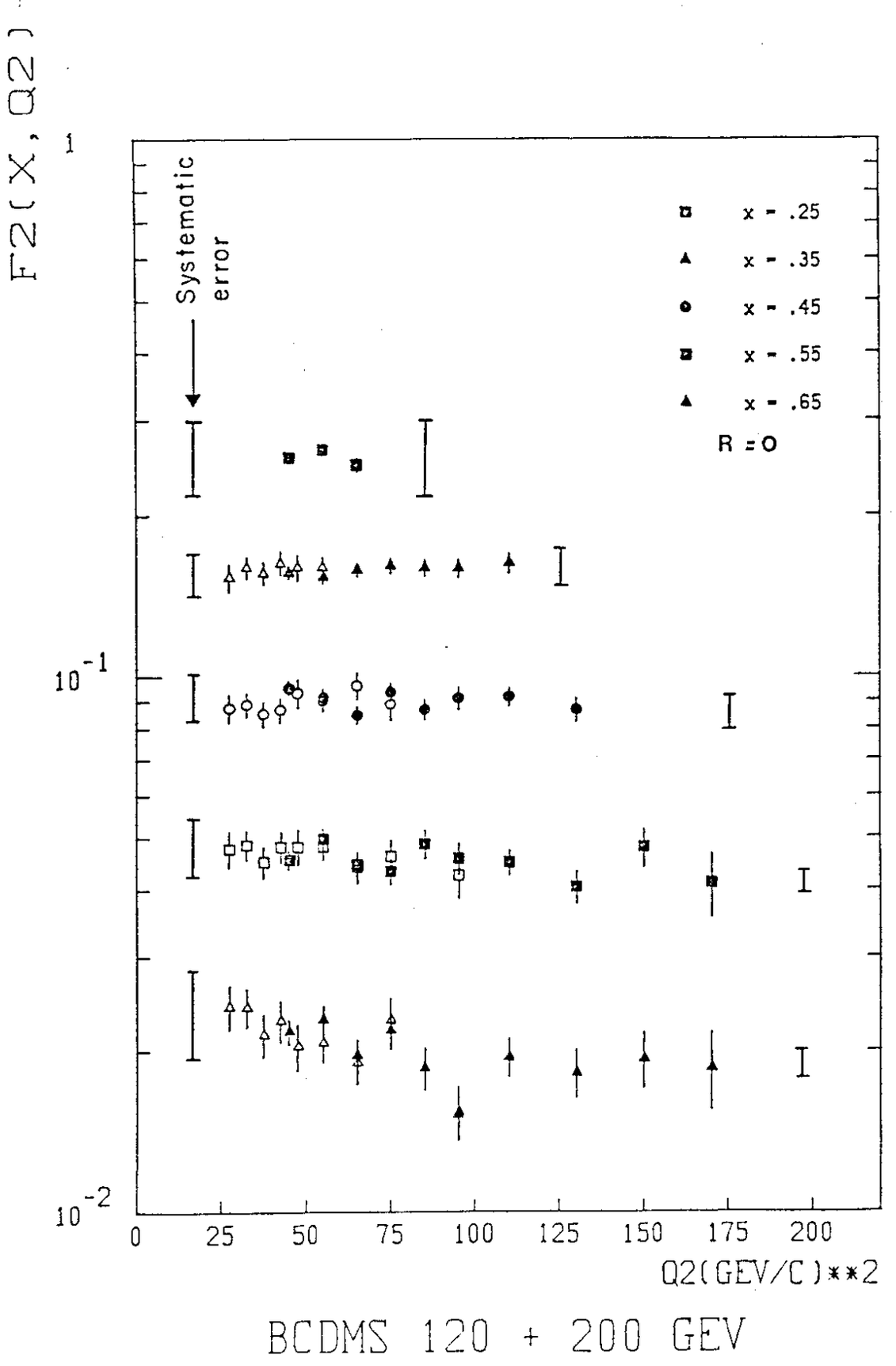

Fig. 7a $F_2(x,Q^2)$ measured at 120 GeV (open symbols, $Q^2 > 25$ $(GeV/c)^2$) and at 200 GeV (closed symbols, $Q^2 > 40$ $(GeV/c)^2$) given with statistical errors at the bin centres, for R = 0 and not corrected for Fermi motion. The error bars at the edges indicate the estimated systematic uncertainty (see text)

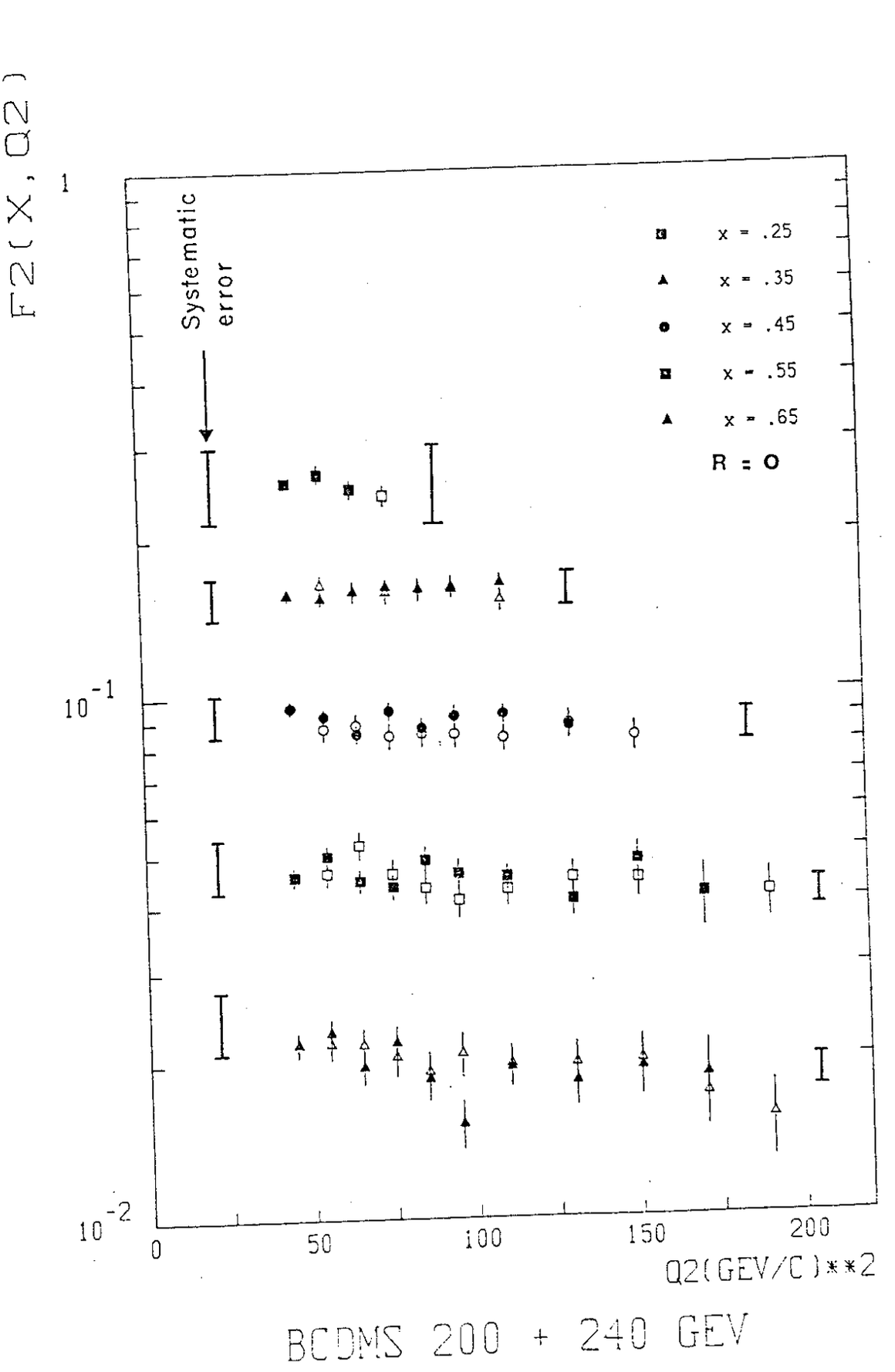

Fig. 7b $F_2(x,Q^2)$ measured at 200 GeV (closed symbols, $Q^2 > 40$ $(GeV/c)^2$) and at 240 GeV (open symbols, $Q^2 > 50$ $(GeV/c)^2$) given with statistical errors at the bin centres, for R = 0 and not corrected for Fermi motion. The error bars at the edges indicate the estimated systematic uncertainty (see text). Whenever above $Q^2 = 50$ $(GeV/c)^2$ only a closed symbol appears, both measurements coincide.

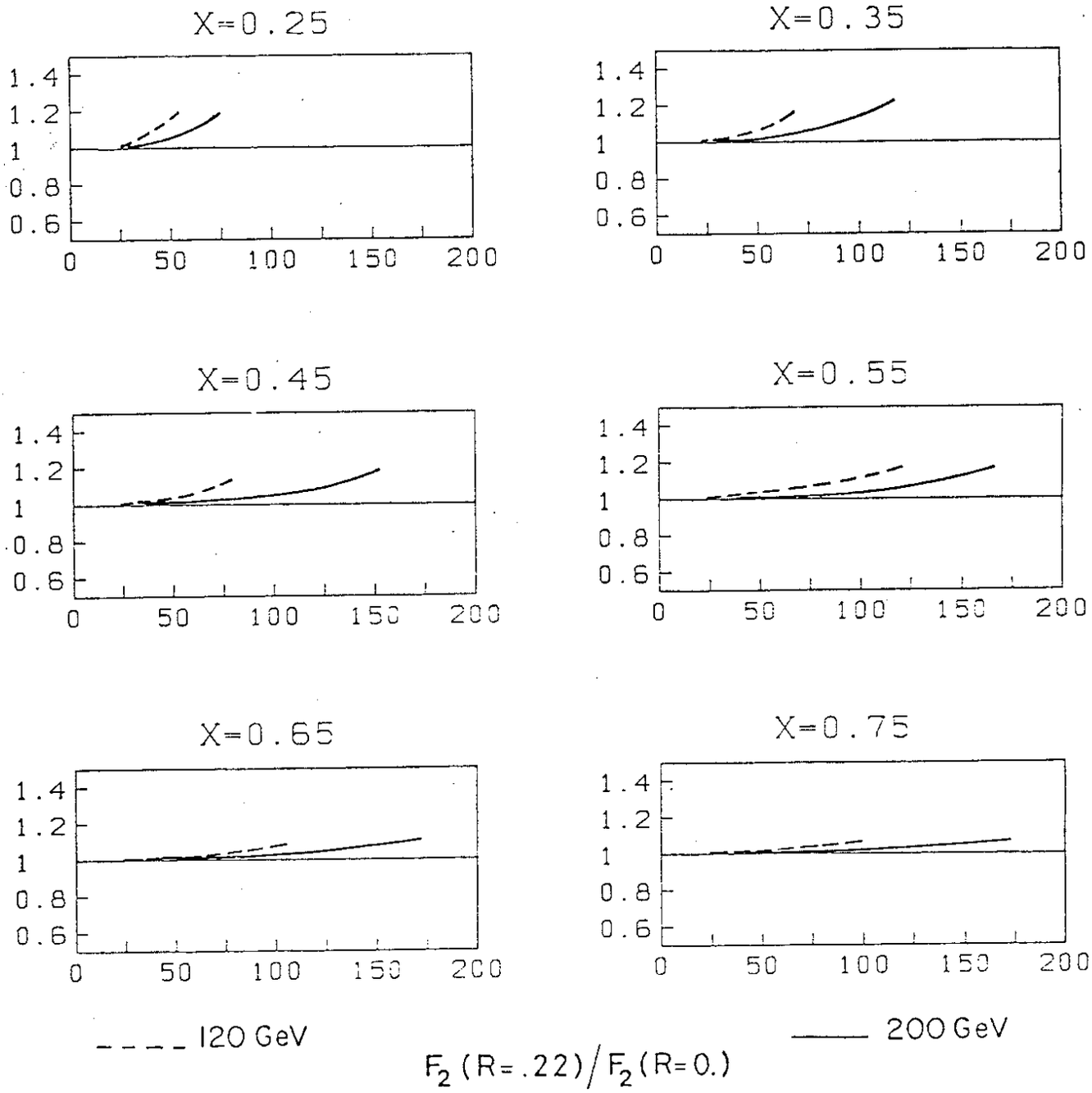

Fig. 8 Effect on F_2 of varying $R = \sigma_L/\sigma_T$ from 0 to 0.22 at 120 GeV (dashed curves) and 200 GeV (solid curves)

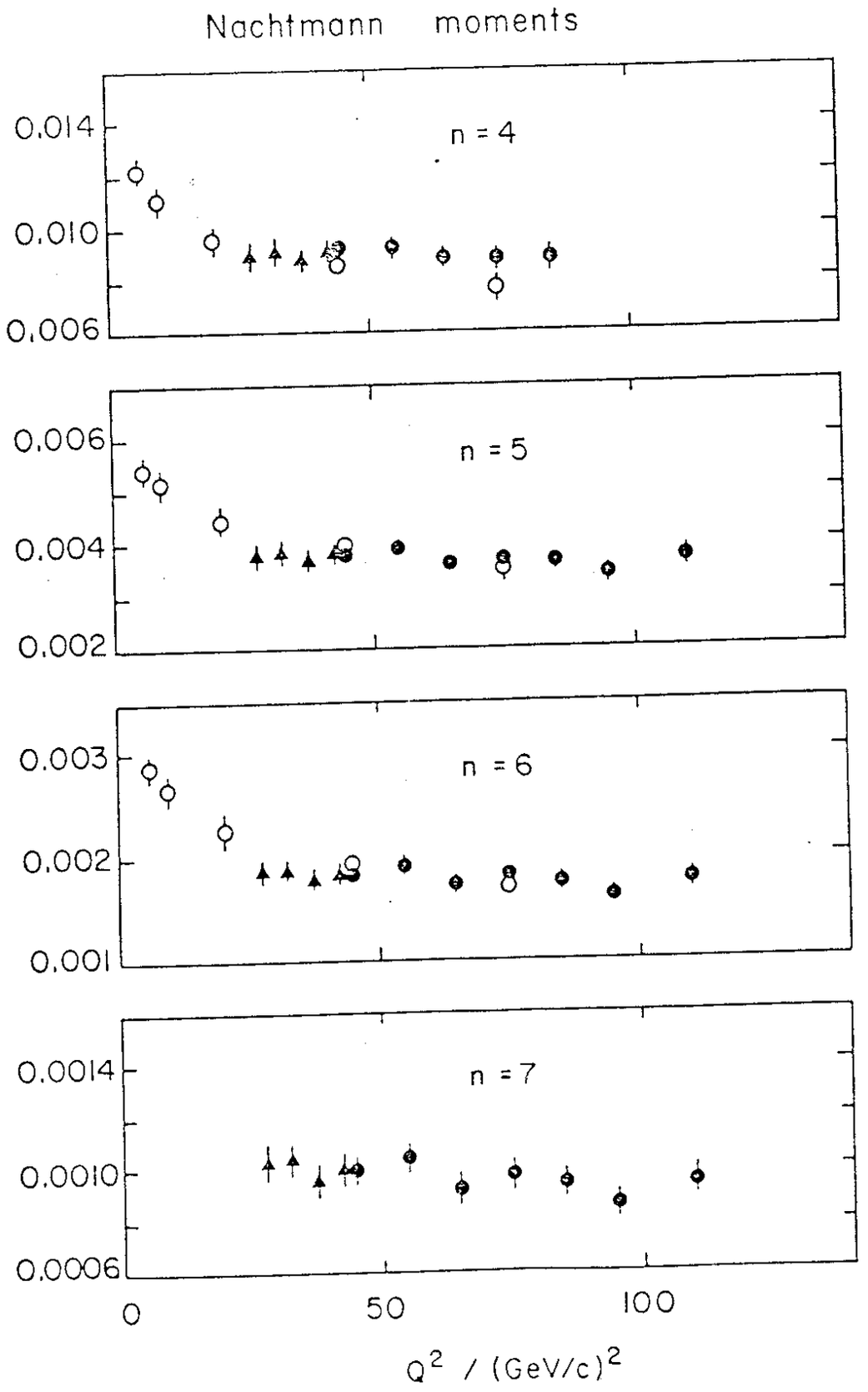

Fig. 9 Nachtmann moments of F_2 at 120 GeV (▲) and 200 GeV (●) for $4 \leq n \leq 7$. The error bars combine the statistical error with the extrapolation uncertainty. Open points: moments of the non-singlet xF_3 times 5/18 as calculated by CDHS[3]